Pseudomomentum Diagnostics for Two-Dimensional Stratified Compressible Flow

DALE R. DURRAN

Department of Atmospheric Sciences, University of Washington, Seattle, Washington

(Manuscript received 20 July 1994, in final form 1 May 1995)

ABSTRACT

Expressions are derived for the local pseudomomentum density in two-dimensional compressible stratified flow and are compared with the expressions for pseudomomentum in two-dimensional Boussinesq and anelastic flow derived by Shepherd and by Scinocca and Shepherd. To facilitate this comparison, algebraically simpler expressions for the anelastic and Boussinesq pseudomomentum are also obtained. When the vertical wind shear in the reference-state flow is constant with height, the Boussinesq pseudomomentum is shown to reduce to a particularly simple form in which the pseudomomentum is proportional to the perturbation vorticity times the fluid-parcel displacement. The extension of these compressible pseudomomentum diagnostics to viscous flow and to three-dimensional flows with zero potential vorticity is also discussed.

An expression is derived for the pseudomomentum flux in stratified compressible flow. This flux is shown to simultaneously satisfy the group-velocity condition for both sound waves and gravity waves in an isothermal atmosphere with a constant basic-state wind speed. Consistent with the earlier results of Andrews and McIntyre, it is shown that for inviscid flow over a topographic barrier, the pseudomomentum flux through the lower boundary is identical to the cross-mountain pressure drag—provided that the flow is steady and that the elevation of the topography returns to its upstream value on the downstream side of the mountain.

1. Introduction

The goal of this paper is to derive expressions for the pseudomomentum and pseudomomentum fluxes in two-dimensional nonrotating (i.e., $f = 0$) stratified compressible flow. These new expressions for the pseudomomentum and pseudomomentum fluxes in compressible flow will be compared with results previously obtained for the two-dimensional Boussinesq and anelastic equations by Shepherd (1990) and by Scinocca and Shepherd (1992), hereafter referred to as S90 and SS92 respectively. Algebraically simpler versions of the expressions provided in S90 and SS92 are obtained in order to facilitate this comparison. Durran (1995) employs the pseudomomentum diagnostics derived in this paper to analyze the interaction of numerically simulated mountain waves with the mean flow.

The derivation of these pseudomomentum diagnostics utilizes noncanonical Hamiltonian theory and follows the general approach outlined in the excellent review by Shepherd (S90) and subsequently employed in SS92 to determine wave activity diagnostics for the two-dimensional anelastic equations. In particular, we adopt SS92's strategy of identifying the global pseudomomentum invariant in the simplest possible context, using that pseudomomentum invariant to identify a local pseudomomentum density, P, and then set aside the Hamiltonian theory and use the conventional form of the governing equations to determine fluxes whose divergence is $\partial P/\partial t$.

The derivation of a local pseudomomentum density for two-dimensional stratified compressible flow is presented in section 2. In section 3, these new results are compared with the formulas for pseudomomentum in two-dimensional anelastic and Boussinesq flow previously presented in S90 and SS92. Expressions for the pseudomomentum flux in compressible flow are derived and discussed in section 4. The perturbation momentum and pseudomomentum fields in a nonbreaking mountain wave are compared in section 5. The extension of the preceding results to dissipative and three-dimensional flows is discussed in section 6. Practical considerations involved in the computation of these quantities are described in section 7. Section 8 contains the conclusions. Throughout this paper, reference state quantities will be denoted by an overbar and perturbations about that reference state will be denoted by primes. Unless explicitly stated otherwise, it will not be assumed that the perturbations about the reference state are small.

2. Pseudomomentum in 2D stratified compressible flow

As the first step in the derivation of an expression for the pseudomomentum, the equations governing inviscid adiabatic two-dimensional flow,

Corresponding author address: Dr. Dale R. Durran, Department of Atmospheric Sciences, AK-40, University of Washington, Seattle, WA 98195.
E-mail: durrand@atmos.washington.edu

$$\frac{du}{dt} + \frac{1}{\rho}\frac{\partial p}{\partial x} = 0, \tag{1}$$

$$\frac{dw}{dt} + \frac{1}{\rho}\frac{\partial p}{\partial z} = -g, \tag{2}$$

$$\frac{\partial \rho}{\partial t} + \frac{\partial \rho u}{\partial x} + \frac{\partial \rho w}{\partial z} = 0, \tag{3}$$

$$\frac{d\theta}{dt} = 0, \tag{4}$$

are reexpressed in the *symplectic* form

$$\mathbf{U}_t = \mathbf{J}\frac{\delta \mathcal{H}}{\delta \mathbf{U}}. \tag{5}$$

Here, $\mathbf{U}$ is a column vector of the dependent variables, $\mathbf{J}$ is a matrix operator satisfying certain algebraic properties (see S90, p. 293), and $\mathcal{H}$ is the Hamiltonian, or total energy. In our case these quantities are

$$\mathbf{U} = (u \quad w \quad \rho \quad \theta)^{\mathrm{T}},$$

$$\mathbf{J} = \begin{pmatrix} 0 & -\omega/\rho & -\partial/\partial x & \theta_x/\rho \\ \omega/\rho & 0 & -\partial/\partial z & \theta_z/\rho \\ -\partial/\partial x & -\partial/\partial z & 0 & 0 \\ -\theta_x/\rho & -\theta_z/\rho & 0 & 0 \end{pmatrix},$$

and

$$\mathcal{H} = \iint \left\{ \frac{\rho}{2}(u^2 + w^2) + \rho c_v T + \rho g z \right\} dxdz.$$

In the preceding, ω is the vorticity, $\partial u \partial z - \partial w/\partial x$; the subscripts x, z, and t denote partial differentiation, and $\delta\mathcal{H}/\delta\mathbf{U}$ is the functional derivative of $\mathcal{H}$ with respect to $\mathbf{U}$:

$$\frac{\delta \mathcal{H}}{\delta \mathbf{U}} = (\delta\mathcal{H}/\delta u \quad \delta\mathcal{H}/\delta w \quad \delta\mathcal{H}/\delta \rho \quad \delta\mathcal{H}/\delta\theta)^{\mathrm{T}}.$$

The preceding is the two-dimensional equivalent of the symplectic form provided in S90 for three-dimensional compressible stratified flow. The reader is referred to S90 (p. 309) for further details.

If the boundaries of the spatial domain are periodic or the domain is unbounded and the perturbations vanish (with sufficient rapidity) at infinity, Eqs. (1) and (3) may be combined and integrated to show that total momentum

$$\mathcal{M} = \iint \rho u dxdz \tag{6}$$

is conserved.[1] As reviewed in S90, the conservation of $\mathcal{M}$ can also be derived via the Hamiltonian theory using Noether's theorem since the Hamiltonian $\mathcal{H}$ is invariant under translations in x and

$$\mathbf{J}\frac{\delta\mathcal{M}}{\delta\mathbf{U}} = -\mathbf{U}_x.$$

Suppose that some reference state, $\bar{\mathbf{U}}$, is independent of x; then

$$\mathbf{J}\frac{\delta\mathcal{M}}{\delta\mathbf{U}}\bigg|_{\mathbf{U}=\bar{\mathbf{U}}} = -\bar{\mathbf{U}}_x = 0. \tag{7}$$

If, as in many classical problems involving finite-dimensional systems, the governing dynamics were expressible in a canonical Hamiltonian formulation, the matrix operator $\mathbf{J}$ would be nonsingular and the preceding would imply that

$$\frac{\delta\mathcal{M}}{\delta\mathbf{U}}\bigg|_{\mathbf{U}=\bar{\mathbf{U}}} = 0. \tag{8}$$

This relation does *not* hold in most fluid dynamical applications because the Hamiltonian formulation is noncanonical and $\mathbf{J}$ is singular. The failure of $\mathcal{M}$ to satisfy (8) represents a failure of the total momentum of a fluid to inherit all the dynamical properties associated with the total momentum of simpler canonical systems such as a pair of frictionless hockey pucks.

When $\mathbf{J}$ is singular, there exist nontrivial Casimir functionals, $\mathcal{C}$, such that

$$\mathbf{J}\frac{\delta\mathcal{C}}{\delta\mathbf{U}} = 0. \tag{9}$$

According to (7), whenever $\bar{\mathbf{U}}_x = 0$, $\delta\mathcal{M}/\delta\mathbf{U}$ lies within the kernel of $\mathbf{J}$ and, as demonstrated by Littlejohn (1982), there must exist a Casimir $\tilde{\mathcal{C}}$, such that

$$\frac{\delta\tilde{\mathcal{C}}}{\delta\mathbf{U}}\bigg|_{\mathbf{U}=\bar{\mathbf{U}}} = -\frac{\delta\mathcal{M}}{\delta\mathbf{U}}\bigg|_{\mathbf{U}=\bar{\mathbf{U}}}. \tag{10}$$

As noted by McIntyre and Shepherd (1987) (see also S90), the Casimir $\tilde{\mathcal{C}}$ may be used to construct the following expression for the pseudomomentum:

$$\mathcal{P}(\mathbf{U}) = \mathcal{M}(\mathbf{U}) - \mathcal{M}(\bar{\mathbf{U}}) + \tilde{\mathcal{C}}(\mathbf{U}) - \tilde{\mathcal{C}}(\bar{\mathbf{U}}). \tag{11}$$

By construction, $\mathcal{P}$ and $\delta\mathcal{P}/\delta\mathbf{U}$ are both zero when $\mathbf{U} = \bar{\mathbf{U}}$. In addition, $\mathcal{P}$ satisfies Noether's theorem and is, therefore, invariant in time. In short, $\mathcal{P}$ behaves like the conventional perturbation momentum in a canonical Hamiltonian system.

Once appropriate Casimir functionals have been identified, (11) can be used to obtain specific formulas for the pseudomomentum in two-dimensional compressible flow. A plausible generalization of the Casimir functional for two-dimensional anelastic flow [SS92, Eq. (4.13)] to the case of two-dimensional stratified compressible flow is

[1] Other boundary conditions, and, in particular, the effects of orography, will be considered after determining the basic form of the local pseudomomentum density.

$$\mathcal{C} = \iint [\rho C_1(\theta) + \omega C_2(\theta)]dxdz. \quad (12)$$

To verify that the preceding expression (which does not seem to have been previously recorded in the literature) is indeed a Casimir, note that

$$\delta\mathcal{C} = \iint \left[C_1\delta\rho + \rho\dot{C}_1\delta\theta + C_2\left(\frac{\partial\delta u}{\partial z} - \frac{\partial\delta w}{\partial x}\right) + \omega\dot{C}_2\delta\theta \right] dxdz,$$

where the dots denote ordinary derivatives. Integrating by parts and neglecting the exact differentials, which integrate to zero by the assumed boundary conditions, one obtains

$$\delta\mathcal{C} = \iint [C_1\delta\rho + (\rho\dot{C}_1 + \omega\dot{C}_2)\delta\theta - \dot{C}_2\theta_z\delta u + \dot{C}_2\theta_x\delta w]dxdz.$$

It follows that

$$\frac{\delta\mathcal{C}}{\delta\mathbf{U}} = (-\dot{C}_2\theta_z \quad \dot{C}_2\theta_x \quad C_1 \quad \rho\dot{C}_1 + \omega\dot{C}_2)^{\mathrm{T}}$$

and that $\mathcal{C}$ satisfies the Casimir condition (9).

The exact form of the undetermined functions $C_1(\theta)$ and $C_2(\theta)$ appearing in the pseudomomentum functional are determined by the condition (10), which in the current example is equivalent to the four scalar equations

$$\bar{\rho} - \dot{C}_2(\bar{\theta})\bar{\theta}_z = 0, \quad (13)$$

$$\bar{\theta}_x = 0, \quad (14)$$

$$\bar{u} + C_1(\bar{\theta}) = 0, \quad (15)$$

$$\bar{\rho}\dot{C}_1(\bar{\theta}) + \bar{u}_z\dot{C}_2(\bar{\theta}) = 0. \quad (16)$$

Here, and throughout this paper, the overbars represent horizontally uniform reference state quantities that may be specified arbitrarily and need not be equal to horizontal spatial means. Equation (14) is trivially satisfied by our previous assumption that $\bar{U}_x = 0$. Specific expressions for C_1 and C_2 are conveniently formulated in terms of an auxiliary function $\bar{z}(\theta)$, which is the height in the reference flow at which the reference-state potential temperature $\bar{\theta}$ is equal to θ. Assuming that the reference state is stably stratified (which will be the case in all examples considered here), $\bar{z}(\theta)$ is always single valued. Noting that $\bar{z}(\bar{\theta}) = z$, one may easily show that (13) and (15) are satisfied by choosing

$$C_1(\theta) = -\bar{u}(\bar{z}(\theta)) \equiv -\bar{u}(\theta),$$

and

$$C_2(\theta) = \int^{\bar{z}(\theta)} \bar{\rho}(\zeta)d\zeta.$$

It remains to verify that these expressions for C_1 and C_2 also satisfy (16). Substituting for $C_1(\bar{\theta}) = -\bar{u}(\bar{\theta})$ in (16) one obtains

$$-\bar{\rho}\frac{d\bar{u}}{dz}\frac{dz}{d\bar{\theta}} + \frac{d\bar{u}}{dz}\dot{C}_2(\bar{\theta}) = 0,$$

which is equivalent to (13) and thus satisfied by our chosen C_2.

The pseudomomentum functional for two-dimensional compressible flow is obtained by substituting the preceding expressions for C_1 and C_2 into (12) and then inserting (12) and (6) into (11). After some simplification, the result may be written

$$\mathcal{P} = \iint \left[\rho[u - \bar{u}(\theta)] + \omega\int_z^{\bar{z}(\theta)} \bar{\rho}(\zeta)d\zeta + \omega'\int^z \bar{\rho}(\zeta)d\zeta \right] dxdz,$$

where primed quantities denote perturbations about the horizontally uniform reference state and, unless otherwise noted, these perturbations may be finite amplitude. The last term in the preceding formula can be transformed into a form more suitable for computation by noting that

$$\iint \left(\frac{\partial u'}{\partial z} - \frac{\partial w'}{\partial x}\right)\int^z \bar{\rho}(\zeta)d\zeta dxdz$$

$$= \iint \left[\frac{\partial}{\partial z}\left(u'\int^z \bar{\rho}(\zeta)d\zeta\right) - \bar{\rho}u' - \frac{\partial}{\partial x}\left(w'\int^z \bar{\rho}(\zeta)d\zeta\right) \right] dxdz$$

$$= -\iint \bar{\rho}u'dxdz,$$

where the exact differentials integrate to zero by the assumed boundary conditions. The pseudomomentum functional for two-dimensional compressible flow may, thus, be reexpressed as

$$\mathcal{P} = \iint \left[(\rho - \bar{\rho})u' + \rho[\bar{u}(z) - \bar{u}(\theta)] + \omega\int_z^{\bar{z}(\theta)} \bar{\rho}(\zeta)d\zeta \right] dxdz. \quad (17)$$

Our main interest is not in the global pseudomomentum functional $\mathcal{P}$, but the local pseudomomentum density

$$P = \rho'u' + \rho[\bar{u}(z) - \bar{u}(\theta)] + \omega\int_z^{\bar{z}(\theta)} \bar{\rho}(\zeta)d\zeta, \quad (18)$$

whose domain integral is $\mathcal{P}$. This is completely analogous to the more familiar situation with conventional momentum, in which the primary focus is on the local perturbations rather than their domain average $\mathcal{M}$. Thus, in the remainder of this paper, ''pseudomomentum'' will refer to the local pseudomomentum density, P, rather than its global integral $\mathcal{P}$.

3. Comparison with expressions for Boussinesq and anelastic flow

It is useful to compare the preceding expression for pseudomomentum in two-dimensional compressible flow to the corresponding expressions for the two-dimensional Boussinesq and anelastic equations. SS92 provide a relatively complex formula for the anelastic pseudomomentum, P_a [their (6.10)] that was designed to show $\mathcal{P}_a$ in an obviously quadratic form. A simpler expression, which may be more easily compared with (18), can be obtained by returning to SS92's (6.8) and noting that

$$\int_0^{\theta'} S(\overline{\theta} + \eta)d\eta = \int_{\overline{\theta}}^{\theta} \frac{d\overline{u}}{d\overline{\theta}} d\theta = \overline{u}(\theta) - \overline{u}(\overline{\theta}) = \overline{u}(\theta) - \overline{u}(z).$$

Substituting the preceding in SS92's (6.8), the anelastic pseudomomentum density is seen to be

$$P_a = \overline{\rho}[\overline{u}(z) - \overline{u}(\theta)] + \omega \int_z^{\overline{z}(\theta)} \overline{\rho}(\zeta)d\zeta, \quad (19)$$

where the horizontally uniform reference density, $\overline{\rho}(z)$, has replaced $\rho_0(z)$ in the SS92 notation. Here P_a differs from P in that it omits those terms involving perturbation density; this, of course, is consistent with the fundamental approximation used to derive the anelastic system. The local pseudomomentum density in incompressible Boussinesq flow may be expressed in an even simpler form:

$$P_b = \rho_0[\overline{u}(z) - \overline{u}(\rho)] + \rho_0\omega[\overline{z}(\rho) - z], \quad (20)$$

where ρ_0 is a constant reference density, $\overline{z}(\rho)$ is the height in the reference flow where $\overline{\rho} = \rho$, and $\overline{u}(\rho) \equiv \overline{u}(\overline{z}(\rho))$. (Recall that ρ is conserved along trajectories in incompressible Boussinesq flow.) The expression (20) is also simpler than those noted previously in S90 and SS92, which were, once again, designed to be obviously quadratic. The form given here may be obtained from Eqs. (5.10)–(5.12) of S90 after noting that $C_1(R) = -U(Z_0(R))$. (The S90 result must also be multiplied by ρ_0.) A comparison of (19) and (20) shows that, as one might expect, the Boussinesq form neglects those terms retained in the anelastic system involving variations in reference-state density.

A particularly simple expression is available for the *finite-amplitude* Boussinesq pseudomomentum when the reference-state wind shear is constant with height. Let ψ' be the vertical displacement of an air parcel from its level in the reference flow, $z - \overline{z}(\rho)$. Then by the assumption that the reference-state wind shear is constant, (20) reduces to

$$P_b = \rho_0(\overline{\omega}\psi' - \omega\psi') = -\rho_0\omega'\psi'. \quad (21)$$

A concise description of the Boussinesq pseudomomentum with respect to a constant-shear reference state is, therefore, that *the pseudomomentum is proportional to the perturbation vorticity times the fluid-parcel displacement.* According to (21), the domain-integrated pseudomomentum (with respect to a constant-shear reference state) is closely related to the fluid impulse (Batchelor 1967, p. 529)

$$-\iint \rho_0\omega z dx dz.$$

Assuming the relevant integrals are convergent, any change in the domain-integrated fluid impulse is identical to the change in the domain-integrated horizontal momentum.

As an illustration of the distinction between perturbation momentum and pseudomomentum, note that the local pseudomomentum density is zero throughout any Boussinesq fluid in which all the isosteric surfaces are horizontal. This result is independent of the instantaneous velocity field and it also applies to finite-amplitude disturbances, provided one uses the horizontally uniform isosteric surfaces to define the reference-state density. When $\overline{\rho}$ is so defined, $\overline{z}(\rho) = \overline{z}(\overline{\rho}) = z$ and (20) is zero. In addition, since the global integral of the pseudomomentum density, $\mathcal{P}_b$, is conserved, it will remain zero even if P_b changes as the isosteric surfaces immediately deform in response to a nontrivial vertical velocity field. A simple example of this type is provided by a standing gravity wave whose streamfunction has the form

$$\sin(kx + lz)\sin\nu t.$$

There is no preferred sense of propagation to this disturbance, and its pseudomomentum, averaged over one horizontal wavelength, is always zero. Further discussion of the relationship between momentum and pseudomomentum is provided in McIntyre (1981).

4. Pseudomomentum fluxes

To determine expressions for the pseudomomentum fluxes, we follow the approach in S90 and SS92, in which Hamiltonian theory is now laid aside and the governing equations (1)–(4) are used in their conventional form to obtain an equation for the local time tendency of P. Before presenting the results for compressible flow, consider the simpler Boussinesq case, for which it is convenient to define

$$H_b = \overline{z}(\rho) - z \quad \text{and} \quad \hat{P}_b = P_b + \rho_0 u'.$$

The Boussinesq pseudomomentum in an adiabatic, inviscid flow satisfies

$$\frac{\partial P_b}{\partial t} + \nabla \cdot \mathbf{F}_b = 0, \tag{22}$$

where the Boussinesq pseudomomentum fluxes may be written as

$$\mathbf{F}_b = \left(u\hat{P}_b - \frac{\rho_0}{2}(u^2 - \bar{u}^2 + w^2) - g\frac{H_b^2}{2}\frac{\partial \rho}{\partial z}, w\hat{P}_b + g\frac{H_b^2}{2}\frac{\partial \rho}{\partial x} \right). \tag{23}$$

The preceding may be derived from Eq. (6.22) of SS92 by noting that

$$\frac{\partial H_b}{\partial x} = \frac{d\bar{z}}{d\rho}\frac{\partial \rho}{\partial x}, \quad \frac{\partial H_b}{\partial z} = \frac{d\bar{z}}{d\rho}\frac{\partial \rho}{\partial z} - 1,$$

and, therefore,

$$-\frac{\partial}{\partial x}\left(\int_0^\rho [\bar{z}(\tilde{\rho}) - z] d\tilde{\rho} \right) = -H_b \frac{\partial \rho}{\partial x} = \frac{\partial}{\partial x}\left(-\frac{H_b^2}{2}\frac{\partial \rho}{\partial z} \right) + \frac{\partial}{\partial z}\left(\frac{H_b^2}{2}\frac{\partial \rho}{\partial x} \right).$$

The various expressions for $\mathbf{F}_b$ are not unique as any nondivergent vector field could be added to $\mathbf{F}_b$ and the resulting sum would still satisfy (22). SS92 recommend avoiding this ambiguity by requiring $\mathbf{F}_b$ to satisfy the "group-velocity condition" that in the limit of small-amplitude waves

$$\langle\langle \mathbf{F}_b \rangle\rangle = \mathbf{c}_g \langle\langle P_b \rangle\rangle,$$

where $\mathbf{c}_g$ is the group-velocity vector, the double angle brackets denote an average over one phase of the wave, and the equality holds only through the leading order in the perturbation variables. Although (23) is in a different form from that given in SS92, it's small-amplitude limit is identical to the small-amplitude limit of the flux given in SS92 [their Eq. (6.20)], and as demonstrated in SS92, this small-amplitude flux satisfies the group-velocity condition. Thus, (23) must also satisfy the group-velocity condition.

Now consider compressible flow, for which it is convenient to define the quantities

$$H = \int_z^{\bar{z}(\theta)} \bar{\rho}(\zeta) d\zeta$$

and $\hat{P} = P + \bar{\rho}u'$. Then the local change in the pseudomomentum in two-dimensional inviscid adiabatic flow is governed by

$$\frac{\partial P}{\partial t} + \nabla \cdot \mathbf{F} = 0, \tag{24}$$

where the pseudomomentum flux vector, $\mathbf{F}$, may be concisely written in the particular form

$$\mathbf{F}_1 = \left(u\hat{P} + p - \bar{\rho}\left(\frac{u^2 + w^2}{2} + c_p T \right) + TH\frac{\partial \eta}{\partial z}, \quad w\hat{P} - TH\frac{\partial \eta}{\partial x} \right), \tag{25}$$

and η is the entropy, defined such that

$$\eta = c_p \ln\theta + \text{constant}.$$

Once again, the preceding expression for $\mathbf{F}$ is not unique and, in fact, it does not satisfy the group-velocity condition. A different form for the pseudomomentum flux, which does appear to satisfy the group-velocity condition, is

$$F_{(x)} = u\hat{P} - \frac{\bar{\rho}(z)}{2}(u^2 - \bar{u}^2 + w^2) + \frac{g}{\bar{\theta}}\int_{\bar{\theta}}^{\theta} H(\zeta)d\zeta + p' - c_p\bar{\rho}\,\theta\pi' + c_p\pi' H\frac{\partial \theta}{\partial z} \tag{26}$$

$$F_{(z)} = w\hat{P} - c_p\pi' H\frac{\partial \theta}{\partial x}, \tag{27}$$

where $F_{(x)}$ and $F_{(z)}$ are the x and z components of $\mathbf{F}$, π' is the deviation of the nondimensional pressure $(p/p_0)^{R/c_p}$ from its reference-state value, and p_0 is a constant, typically 10^5 Pa. A demonstration that the fluxes (26) and (27) satisfy the pseudomomentum budget equation (24) is provided in appendix A. The group-velocity condition is verified in appendix B for the case of linear waves in an isothermal atmosphere with a uniform mean flow. Unlike the Boussinesq and anelastic systems, compressible stratified flow supports two distinctly different types of waves and it is worth noting that the preceding fluxes simultaneously satisfy the group-velocity conditions for both sound waves and gravity waves.

The pseudomomentum fluxes identified in this paper have the property that, at steady-state, the pseudomomentum flux of $\mathbf{F}$ across any streamline is identical to the conventional momentum flux across the same streamline provided that the difference between the upstream and downstream elevation of the streamline vanishes as $x \to \infty$. This result is consistent with the relationship between the fluxes of momentum and pseudomomentum previously noted by Andrews and McIntyre (1978) and McIntyre (1981). In particular, the requirements for zero net streamline displacement and steady-state flow appear consistent with the necessary criteria for satisfaction of McIntyre's "pseudomomentum rule" (McIntyre 1981, p. 342). To supplement the general discussion presented by Andrews and McIntyre, the following will provide a more detailed derivation of the relationship between the fluxes of momentum and pseudomomentum for the specific case of two-dimensional stratified flow. Begin by considering the flux of some vector field $\mathbf{G}$ across an arbitrary streamline, let the height of the streamline be given by $z_s(x)$ and let n be the upward-directed unit vector normal to the streamline. Then the total cross-streamline flux is

$$\int_{-\infty}^{\infty} \mathbf{G}\cdot\mathbf{n}ds = \int_{-\infty}^{\infty} \left[-G_{(x)} \frac{dz_s}{dx} + G_{(z)} \right] dx, \quad (28)$$

where s is the distance along the arc of the streamline, and $G_{(x)}$ and $G_{(z)}$ are the components of $\mathbf{G}$ parallel to the coordinate axes. A specific expression for the vector momentum flux may be obtained by writing the horizontal momentum equation in flux form,

$$\frac{\partial \rho u}{\partial t} + \nabla\cdot(\rho u \mathbf{v} + p\mathbf{i}) = 0,$$

where $\mathbf{v}$ is the velocity vector and $\mathbf{i}$ is the unit vector parallel to the x axis. The advective fluxes, $\rho u\mathbf{v}$, make no contribution to the cross-streamline flux, so it follows from (28) that the cross-streamline momentum flux is equal to the pressure drag on the same streamline:

$$-\int_{-\infty}^{\infty} p \frac{dz_s}{dx} dx. \quad (29)$$

Now consider the transport across steady streamlines that would be generated by pseudomomentum fluxes expressed in the concise form (25). The advective contributions $\hat{P}\mathbf{v}$ are once again zero. The contribution from the last term in each component of (25) may be written

$$\int_{-\infty}^{\infty} TH\mathbf{j}\cdot(\nabla\eta \times \mathbf{n})dx,$$

which is zero since the isentropes are parallel to the streamlines in steady-isentropic flow. The cross-streamline pseudomomentum flux thus reduces to

$$-\int_{-\infty}^{\infty} \left[p - \bar{\rho}\left(\frac{u^2 + w^2}{2} + c_pT\right) \right] \frac{dz_s}{dx} dx.$$

Since the flow is assumed steady, the Bernoulli relation

$$\frac{u^2 + w^2}{2} + c_pT + gz = B_0,$$

in which B_0 is constant along the streamline, may be used to rewrite the preceding integral as

$$-\int_{-\infty}^{\infty} p \frac{dz_s}{dx} dx - \int_{-\infty}^{\infty} \bar{\rho}(gz_s - B_0) \frac{dz_s}{dx} dx.$$

The second integral evaluates as zero provided the perturbations in z_s vanish as $x \to \pm\infty$, because $\bar{\rho}$ depends only on z_s. Thus, the cross-streamline momentum and pseudomomentum fluxes are identical and equal to the pressure drag exerted on any steady streamline provided that the difference between the upstream and downstream elevations of the streamline vanishes as $x \to \pm\infty$.[2]

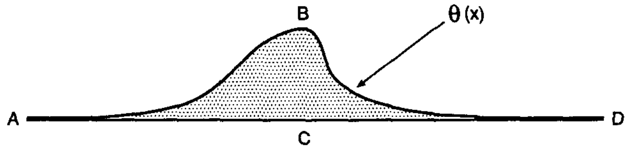

FIG. 1. Steady streamline $\theta(x)$ and horizontal line of zero vertical displacement bounding a closed portion of the x–z domain.

To verify that the preceding result also applies to the form of the pseudomomentum flux that satisfies the group-velocity condition, note that the vertical fluxes $F_{1(z)}$ in (25) and $F_{(z)}$ in (27) differ by the term

$$c_p\bar{\pi}H\frac{\partial\theta}{\partial x} = \frac{\partial}{\partial x}\left(c_p\bar{\pi}(z)\int_{\bar{\theta}}^{\theta} H(\zeta, z)d\zeta\right), \quad (30)$$

whose horizontal integral is zero provided the flow is adiabatic and the streamline displacements vanish as $x \to \pm\infty$. Now consider the pseudomomentum budget in the stippled region shown in Fig. 1, which lies between the steady streamline ABD and the horizontal line of zero vertical displacement ACD, toward which the streamline asymptotes as $x \to \pm\infty$. For simplicity, suppose that the streamline lies entirely above the horizontal line ACD (this argument may easily be extended to handle any number of intersections between the streamline and the line of zero displacement). The net flux into this region is determined by the difference between the fluxes across the streamline and the horizontal line of zero displacement. Since the net flux uniquely determines the pseudomomentum tendency, and since, by the vanishing of the horizontal integral of (30), the total "concise" flux $\mathbf{F}_1$ across ACD is equal to the total "group velocity" flux $\mathbf{F}$ across the same line, the total fluxes of $\mathbf{F}_1$ and $\mathbf{F}$ across the steady streamline must also be identical and equal to the pressure drag on that streamline.

In inviscid flow over topography, the mountain contour is always a steady streamline. The only aspect of the preceding derivation that requires the flow, as opposed to the streamline, to be steady is the neglect of the local time-tendency of pressure in the general time-dependent Bernoulli relation

$$\frac{d}{dt}\left(\frac{u^2 + w^2}{2} + \frac{p}{\rho} + c_vT + gz\right) = \frac{1}{\rho}\frac{\partial p}{\partial t}. \quad (31)$$

[2] A similar argument may be used to show that the cross-streamline Boussinesq pseudomomentum flux (23) is equal to the cross-streamline momentum flux provided the flow is steady and the difference between the upstream and downstream elevations of the streamline vanishes as $x \to \pm\infty$.

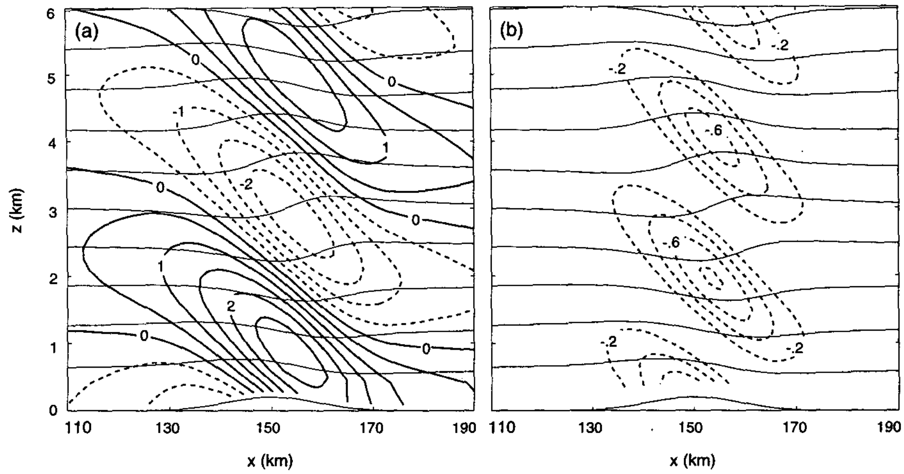

FIG. 2. Isentropes of potential temperature (thin lines, contour interval 2.5 K) plotted at $t = 30\,000$ s, with (a) perturbation horizontal momentum, $\rho u - \bar{\rho}\bar{u}$, (contour interval 0.5 kg m^{-2} s^{-1}) and (b) pseudomomentum (contour interval 0.2 kg m^{-2} s^{-1}).

Evidence from the numerical simulations (see Fig. 4) suggests that, in spite of the abrupt numerical start up procedure,[3] the local pressure perturbations along the mountain slopes quickly become sufficiently steady so that the right side of (31) can be neglected. As a consequence, the pseudomomentum flux through the lower boundary was very well approximated by the cross-mountain pressure drag throughout all but the very beginning of each simulation. Moreover, the abrupt model start up is a much more severe test of the steady-state Bernoulli approximation than that which would be encountered in real atmospheric flows, where the temporal changes associated with mountain wave development occur much more slowly. Thus, one might expect the cross-mountain pressure drag to be an even better approximation to the pseudomomentum flux in real world applications. The wave-induced cross-mountain pressure drag may, therefore, be interpreted as the ultimate source of either the decelerative momentum or pseudomomentum perturbations that are transported aloft by vertically propagating gravity waves.

5. Mountain waves

The true potential of the preceding pseudomomentum diagnostics is most clearly demonstrated in cases where breaking mountain waves exert a "drag" on the flow, and such cases are discussed in Durran (1995). Nevertheless, a useful comparison of pseudomomentum and perturbation momentum diagnostics can be obtained by examining a case of moderate amplitude mountain waves propagating vertically through an atmosphere with constant wind speed and stability. In the case to be examined here, $N = 0.012$ s^{-1}, $u_0 = 8$ ms^{-1}, and the mountain is given by

$$z_s(x) = \begin{cases} h_0[1 + \cos(\pi x/b)]^4/16, & \text{if } |x| \leq b, \\ 0, & \text{otherwise} \end{cases} \quad (32)$$

with $h_0 = 200$ m and $b = 40$ km. The preceding is similar to a Witch of Agnesi with halfwidth $b/4$, but has the advantage that the topography drops to zero a finite distance from the crest. In this case, the nonlinearity parameter, $Nh_0/\bar{u}$, is 0.3 and the wave dynamics are almost linear (Lilly and Klemp 1979).

The results presented in Figs. 2 through 4 were obtained using a time-dependent nonlinear nonhydrostatic numerical model that generates approximate solutions to the full compressible equations of motion. The total numerical domain was 300 km wide and 12 km deep, and the mountain was centered at $x = 150$ km. The horizontal and vertical grid intervals were 750 m and 167 m; the large and small time steps were 10 s and 1.25 s. Further details of the numerical model are provided in Durran (1995).

The perturbation momentum and pseudomomentum fields in the central portion of the domain are shown in Fig. 2. The sign of the perturbation momentum field alternates as the phase of the wave changes with height, whereas the pseudomomentum is everywhere negative. The maxima in the pseudomomentum field are found in those regions where the product of the streamline displacement and the perturbation vorticity is maximized, and those regions are 90° out of phase with the maxima in the perturbation momentum field. Since it is second order in the perturbation amplitude, the pseudomomentum decays more rapidly upstream and downstream of the mountain than does the perturbation

[3] The flow is accelerated from rest to its "upstream" value, and gravity is increased from 0 to 9.8 m s^{-2} over a period 800 s.

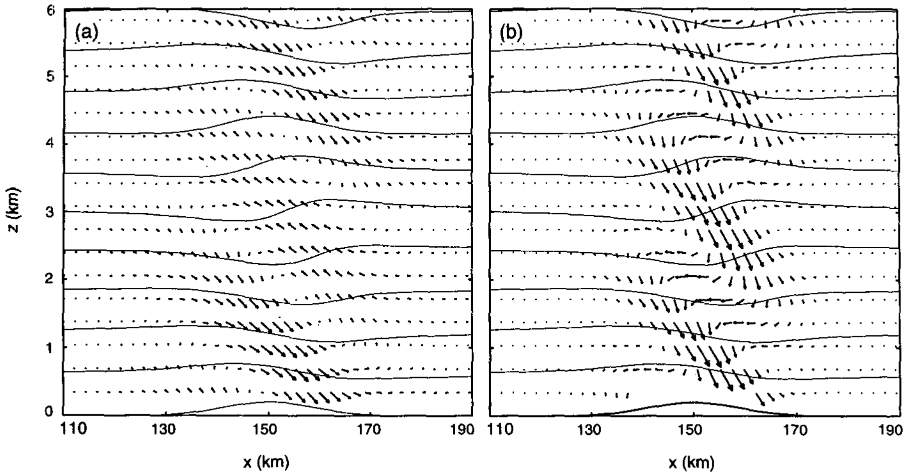

FIG. 3. Isentropes of potential temperature (contour interval 2.5 K) plotted at $t = 30\,000$ s, with (a) perturbation momentum flux vectors and (b) pseudomomentum flux vectors. The vectors are plotted on a coarse mesh consisting of every third horizontal grid point and every second vertical grid point.

momentum, which is a first-order quantity. Although the steady-state pseudomomentum field is everywhere negative, the pseudomomentum is not a negative-definite quantity. Waves propagating to the right relative to the mean flow have positive pseudomomentum, and such waves did appear early in the simulation as transients that subsequently propagated through the downstream boundary as the flow approached steady state. The steady-state pseudomomentum field shown in Fig. 2b is qualitatively similar to that obtained by Scinocca and Peltier (1994), who calculated pseudomomentum perturbations associated with Long's solution for Boussinesq flow over a Witch of Agnesi mountain.

Perturbation momentum and pseudomomentum flux vectors associated with this wave are shown in Fig. 3. The perturbation momentum vector is that obtained by writing the conventional x-momentum equation in the form

$$\frac{\partial}{\partial t}(\rho u - \bar{\rho}\bar{u}) + \frac{\partial}{\partial x}(\rho u^2 - \bar{\rho}\bar{u}^2 + p') + \frac{\partial}{\partial z}\rho uw = 0.$$

The pseudomomentum flux vector is given by (26) and (27). Both vector fields suggest a downward flux into the mountain, and the horizontal-domain average of the vertical component of both fluxes is downward and almost constant with height. The pseudomomentum flux is, however, far more useful for visualizing the downward transport, particularly near the 3-km level, where the strongest momentum flux vectors are directed upward. (The horizontal-domain-averaged vertical momentum flux at the 3-km level is nevertheless downward since the localized region of strong upward momentum flux is compensated by a weak downward flux upstream and downstream of the mountain.)

Finally, the time evolution of the cross-mountain pressure drag is compared with the time evolution of the pseudomomentum flux through the lower boundary in Fig. 4. The flow is gradually accelerated from rest, and the gravitational constant is gradually increased from 0 to 9.8 ms^{-2} over the first 800 s. Except during this period of model initialization, the cross-mountain pressure drag and the total pseudomomentum flux through the lower boundary are in almost perfect agreement. Even during the period of model initialization, when the flow is very unsteady, the agreement between the two curves remains reasonably good. The drag never becomes perfectly steady and both curves de-

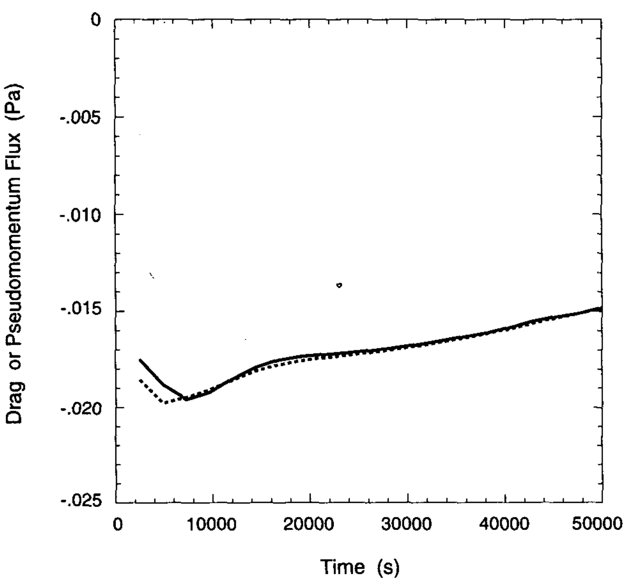

FIG. 4. Cross-mountain pressure drag (solid curve) and total pseudomomentum flux through the lower boundary (dashed curve) plotted as a function of time.

crease slowly with time. As discussed by Klemp and Durran (1983), this temporal variation appears to arise from the erroneous specification of a radiation boundary condition at some *finite* height above the mountain.[4] In any event, the slight time evolution of the pressure drag is useful in the present context, since it further demonstrates that the pseudomomentum flux through the lower boundary may be well approximated by the cross-mountain pressure drag even when the flow is not perfectly steady.

6. Extension to dissipative and 3D flows

It is not possible for a numerical model to explicitly resolve all the relevant scales of motion in turbulent high-Reynolds-number flow. The influence of subgrid-scale turbulent motion on the resolved flow is, therefore, often incorporated in numerical models through a subgrid-scale turbulence parameterization. Let M_u, M_w, and M_θ denote the terms that would appear on the right sides of (1), (2), and (4) representing the time tendencies generated by subgrid-scale mixing. Rederiving the equation for the rate of change of the local pseudomomentum density while retaining these subgrid-scale mixing terms yields

$$\frac{\partial P}{\partial t} + \nabla\cdot\mathbf{F} = S_p,$$

where S_p, representing the sources and sinks of pseudomomentum, is

$$S_p = \rho' M_u + \left(\bar\rho[\bar z(\theta)]\omega\frac{d\bar z}{d\theta} - \rho\frac{d\bar u}{d\theta}\right)M_\theta + H\left(\frac{\partial M_u}{\partial z} - \frac{\partial M_w}{\partial x}\right). \quad (33)$$

The distribution and effect of S_p in breaking mountain waves is discussed in Durran (1995).

The preceding results pertain to two-dimensional flow; in order to generalize them to three-dimensional flows, one needs suitable expressions for the pseudomomentum, which must be generated from the family of Casimir functionals for three-dimensional flow. S90 notes that the Casimirs for three-dimensional compressible flow have the general form

$$\iiint \rho C(\theta, q)\,dx\,dy\,dz,$$

where q is the Ertel potential vorticity

$$q = \frac{\boldsymbol{\omega}\cdot\nabla\theta}{\rho},$$

and $\boldsymbol{\omega}$ is the three-dimensional vorticity vector. The extent to which the Casimir functionals for two-dimensional compressible flow fail to serve as Casimirs for the three-dimensional problem can be determined by substituting (12) into (9), which yields

$$\begin{pmatrix} 0 & \omega_3/\rho & -\omega_2/\rho & -\partial/\partial x & \theta_x/\rho \\ -\omega_3/\rho & 0 & \omega_1/\rho & -\partial/\partial y & \theta_y/\rho \\ \omega_2/\rho & -\omega_1/\rho & 0 & -\partial/\partial z & \theta_z/\rho \\ -\partial/\partial x & -\partial/\partial y & -\partial/\partial z & 0 & 0 \\ -\theta_x/\rho & -\theta_y/\rho & -\theta_z/\rho & 0 & 0 \end{pmatrix} \times \begin{pmatrix} -\dot C_2\theta_z \\ 0 \\ \dot C_2\theta_x \\ C_1 \\ \rho\dot C_1 + \omega_2\dot C_2 \end{pmatrix} = \begin{pmatrix} 0 \\ \dot C_2 q \\ 0 \\ 0 \\ 0 \end{pmatrix},$$

where ω_1, ω_2, and ω_3 are the x-, y-, and z-components of vorticity. Since q is conserved in adiabatic inviscid flow, the preceding suggests that the functionals (12) also serve as Casimirs for the special subset of three-dimensional flows with zero potential vorticity. Moreover, when $q = 0$ and the reference-state isentropes are horizontal, one can define $\bar u(\theta)$ and $\bar z(\theta)$ as in the two-dimensional problem and arrive at the same expression for the pseudomomentum density (18) obtained for two-dimensional flow.

As a consequence, the pseudomomentum diagnostics presented in this paper would appear to be immediately applicable to three-dimensional flows with zero potential vorticity. Schär (1993) has, however, noted that wave breaking can generate potential vorticity anomalies in three-dimensional flows in which the initial potential vorticity was everywhere zero. The immediate effects of such wave breaking can be introduced into the current analysis through source terms in the local pseudomomentum density equation (33), but if patches of nonzero potential vorticity develop in the inviscid flow downstream of a wave breaking region, (18) will no longer serve as an appropriate formula for the calculation of the local pseudomomentum density. A complete discussion of pseudomomentum diagnostics for three-dimensional stratified flow lies beyond the scope of this paper.

7. Computational considerations

The pseudomomentum may be evaluated from gridpoint data in a completely straightforward manner. In practice it was found more convenient to compute P

[4] The problem is not due to the numerical formulation of the boundary condition, but rather with the use of the radiation condition itself.

from equation (A1) of appendix A, rather than (18). The Lagrangian-like quantities $\bar{z}(\theta)$ and $\bar{u}(\theta)$ were evaluated by first defining a one-dimensional array of the reference-state values at the same vertical resolution as the numerical grid (i.e., by defining the values $\bar{z}(\bar{\theta}_j)$, $j = 1, \cdots, N_z$), and then using linear interpolation to obtain arbitrary values of $\bar{z}(\theta)$ and $\bar{u}(\theta)$. The integral in the final term of (35) was evaluated using the trapezoidal rule as

$$\frac{\bar{\rho}[\bar{z}(\theta)] + \bar{\rho}(z)}{2}.$$

No noticeable increase in the accuracy of these calculations was obtained by switching to cubic spline interpolation for $\bar{z}(\theta)$ and $\bar{u}(\theta)$ or subdividing the interval $[z, \bar{z}(\theta)]$ into several subintervals during the trapezoidal integration. It appears that the most serious source of error affecting the evaluation of P is the modest failure of the Eulerian numerical model to perfectly conserve θ along each air parcel trajectory. Nevertheless, as evidenced in Fig. 2 and in Durran (1995), the errors in the along-trajectory conservation of θ are too small to seriously interfere with the evaluation of the pseudomomentum field.

The accurate evaluation of the pseudomomentum-flux divergence seems to be somewhat more difficult, particularly in situations involving quasi-steady mountain waves because the pseudomomentum flux is almost nondivergent (such that values of $F_{(x)}$ exceeded $\nabla \cdot \mathbf{F}$ by factors of 10^5). Although $\mathbf{F}$ is second order in the perturbation variables, $F_{(x)}$ contains two first-order terms, whose difference is second order; that is,

$$p' - c_p \bar{\rho} \theta \pi' = \frac{c_v}{2 c_p \bar{p}} p'^2 + \text{third-order terms.} \qquad (34)$$

The straightforward evaluation of $F_{(x)}$ via (26) appears to pose no problem if one only wishes to compute pseudomomentum flux vectors. When the pseudomomentum flux divergence was required it was, however, found necessary to replace the preceding first-order terms in (26) by the second-order approximation (34) in order to avoid excessive noise in $\nabla \cdot \mathbf{F}$. This is a little unsatisfactory from a pedagogical point of view since third- and higher-order contributions to the total flux are neglected in (34), but retained in the remainder of (26) and (27). At least some of the third-order terms in the vertical pseudomomentum flux are nonnegligible in the strongly nonlinear flows examined in Durran (1995). Nevertheless, in the cases considered in this paper and in Durran (1995), the approximation (34) gave smooth fields of $\nabla \cdot \mathbf{F}$ and an acceptably small residual in the total pseudomomentum budget.

8. Conclusions

Expressions for the local pseudomomentum density (18) and the pseudomomentum fluxes (26) and (27) have been derived for two-dimensional compressible stratified flow. These expressions are applicable at finite amplitude, easily calculable from Eulerian grid-point data, and do not involve WKB approximations or averaging over a wave packet. The formula for pseudomomentum in a compressible flow has been compared with the expressions for pseudomomentum in two-dimensional Boussinesq and anelastic flows previously presented in S90 and SS92. To facilitate this comparison, algebraically simpler expressions for the anelastic and Boussinesq pseudomomentum have been obtained. When the vertical wind shear in the reference state is constant with height, it was demonstrated that the finite-amplitude pseudomomentum in Boussinesq flow is given by the particularly simple formula (21), in which the pseudomomentum is proportional to the perturbation vorticity times the fluid-parcel displacement.

The pseudomomentum fluxes (26) and (27) were shown to satisfy the group-velocity condition for linear waves in an isothermal atmosphere with a constant basic-state wind speed. Moreover, the group-velocity condition is simultaneously satisfied for both types of waves supported by a stratified compressible fluid: sound waves and gravity waves. The relationship between momentum and pseudomomentum fluxes in two-dimensional stratified flow has also been examined and shown to be consistent with the earlier findings of Andrews and McIntyre (1978). For inviscid stratified flow over a topographic barrier, the pseudomomentum flux through the lower boundary is identical to the cross-mountain pressure drag—provided that the flow is steady and that the elevation of the topography returns to its upstream value on the downstream side of the mountain. The assumption of steady flow, which is required only to invoke Bernoulli's theorem, seems to be adequately satisfied even when the large-scale flow over the topography is evolving on a very fast meteorological timescale. Thus, in meteorological applications, the cross-mountain pressure drag may be expected to be identical to the pseudomomentum flux through the topography.

The extension of these pseudomomentum diagnostics to noninviscid and three-dimensional flows has also been considered. The two-dimensional expressions derived in this paper appear to be equally applicable to three-dimensional flows in which the Ertel potential vorticity is everywhere zero. The development of expressions for the pseudomomentum in more general three-dimensional flows is left for future work.

Acknowledgments. This research was conducted while the author was on sabbatical at the Laboratoire d'Aérologie at the Université Paul Sabatier in Toulouse, France. The author is indebted to Evelyne Richard and Daniel Guedalia for providing a stimulating environment for scientific research within the Laboratoire d'Aérologie, and to Ted Shepherd, Doug Lilly, and an anonymous reviewer for their helpful comments. Support for this research was provided by National Science Foundation Grants ATM-9218376 and INT-9116246 and by the French Centre National de Recherche Scientifique, Department Sciences de l'Univers. Computer Services were provided by the National Center for Atmospheric Research, which is sponsored by the National Science Foundation.

APPENDIX A

Derivation of Pseudomomentum Fluxes

It is convenient to rewrite the pseudomomentum (18) in the equivalent form

$$P = \rho[u - \bar{u}(\theta)] - \bar{\rho}(z)u' + \omega H, \qquad (A1)$$

where, as before, $\hat{P} = P + \bar{\rho}(z)u'$ and

$$H = \int_z^{\bar{z}(\theta)} \bar{\rho}(\zeta)d\zeta. \qquad (A2)$$

The local time derivative of each term in (A1) is computed using the governing equations (1)–(4). The results, for the first three terms, may be written

$$\frac{\partial \rho u}{\partial t} = -\frac{\partial}{\partial x}(\rho u^2 + p) - \frac{\partial}{\partial z}(\rho u w), \qquad (A3)$$

$$\frac{\partial \rho \bar{u}(\theta)}{\partial t} = -\frac{\partial}{\partial x}(\rho u \bar{u}(\theta)) - \frac{\partial}{\partial z}(\rho w \bar{u}(\theta)), \qquad (A4)$$

$$\frac{\partial \bar{\rho}(z)u'}{\partial t} = -\frac{\partial}{\partial x}\left(\frac{\bar{\rho}}{2}(u^2 + w^2)\right) - \bar{\rho}w\omega - c_p\bar{\rho}\theta\frac{\partial \pi'}{\partial x}. \qquad (A5)$$

The local time derivative of the remaining term can be evaluated with the aid of the vorticity equation

$$\frac{d\omega}{dt} + \omega\left(\frac{\partial u}{\partial x} + \frac{\partial w}{\partial z}\right) + c_p\left(\frac{\partial \theta}{\partial z}\frac{\partial \pi'}{\partial x} - \frac{\partial \theta}{\partial x}\frac{\partial \pi'}{\partial z}\right) + \frac{g}{\bar{\theta}}\frac{\partial \theta'}{\partial x} = 0,$$

and the relation

$$\frac{\partial H}{\partial t} + u\frac{\partial H}{\partial x} + w\frac{\partial H}{\partial z} + \bar{\rho}w = 0,$$

which may be derived by differentiating (A2) with respect to x, z, and t and substituting the results into the thermodynamic equation. From the two preceding equations, one obtains

$$\frac{\partial \omega H}{\partial t} = -\frac{\partial}{\partial x}(u\omega H) - \frac{\partial}{\partial z}(w\omega H) - \frac{gH}{\bar{\theta}}\frac{\partial \theta'}{\partial x} - \bar{\rho}w\omega - c_pH\left(\frac{\partial \theta}{\partial z}\frac{\partial \pi'}{\partial x} - \frac{\partial \theta}{\partial x}\frac{\partial \pi'}{\partial z}\right). \qquad (A6)$$

Substitution of (A3)–(A6) into the time derivative of (A1) then yields

$$\frac{\partial P}{\partial t} + \frac{\partial}{\partial x}\left(u\hat{P} - \frac{\bar{\rho}}{2}(u^2 + w^2)\right) + \frac{\partial}{\partial z}(w\hat{P}) + \frac{gH}{\bar{\theta}}\frac{\partial \theta'}{\partial x} + \frac{\partial p}{\partial x} - c_p\bar{\rho}\theta\frac{\partial \pi'}{\partial x} + c_pH\left(\frac{\partial \theta}{\partial z}\frac{\partial \pi'}{\partial x} - \frac{\partial \theta}{\partial x}\frac{\partial \pi'}{\partial z}\right) = 0. \qquad (A7)$$

The term involving buoyancy forces can be written as the divergence of a flux by noting that

$$\frac{\partial}{\partial x}\left(\frac{g}{\bar{\theta}}\int_{\bar{\theta}}^{\theta} H(\zeta)d\zeta\right) = \frac{gH}{\bar{\theta}}\frac{\partial \theta'}{\partial x}. \qquad (A8)$$

The terms involving nondimensional pressure (π') can be written in flux form by noting that

$$H\frac{\partial \theta}{\partial x} = \frac{\partial H\theta}{\partial x} - \theta\bar{\rho}(\theta)\frac{d\bar{z}}{d\theta}\frac{\partial \theta}{\partial x},$$

$$H\frac{\partial \theta}{\partial z} = \frac{\partial H\theta}{\partial z} - \theta\bar{\rho}(\theta)\frac{d\bar{z}}{d\theta}\frac{\partial \theta}{\partial z} + \theta\bar{\rho}(z),$$

and thus,

$$\frac{\partial}{\partial x}\left(c_p\pi' H\frac{\partial \theta}{\partial z} - c_p\bar{\rho}\theta\pi'\right) + \frac{\partial}{\partial z}\left(-c_p\pi' H\frac{\partial \theta}{\partial x}\right) = c_pH\left(\frac{\partial \theta}{\partial z}\frac{\partial \pi'}{\partial x} - \frac{\partial \theta}{\partial x}\frac{\partial \pi'}{\partial z}\right) - c_p\bar{\rho}\theta\frac{\partial \pi'}{\partial x}. \qquad (A9)$$

Substituting (A8) and (A9) into (A7) gives $\partial P/\partial t$ as divergence of the flux defined in the text by (26) and (27).

APPENDIX B

Group-Velocity Condition

For the pseudomomentum flux to provide a good indication of wave transport, it should satisfy the group-velocity condition that in the limit of small-amplitude waves

$$\langle\langle \mathbf{F}_b \rangle\rangle = \mathbf{c}_g\langle\langle P_b \rangle\rangle, \qquad (B1)$$

where $\mathbf{c}_g$ is the group-velocity vector and the double angle brackets denote an average over one phase of the wave, or over a wave packet. Ideally, one would like to demonstrate that this relation holds to within the accuracy of the WKB approximation for small-amplitude waves propagating through a slowly varying background flow. The analysis of the full compressible system is, however, sufficiently complex that the following demonstration of the group-velocity condition will be restricted to the case of an isothermal basic state in which the horizontal wind, u_0, is constant.

The leading-order contributions to each side of (B1) are second order in the perturbation fields. As a preliminary step to the evaluation of the second-order contributions to P and $\mathbf{F}$, note that to second order

$$H \approx \bar{\rho}(z) \frac{b'}{N^2},$$

where the perturbation buoyancy and the Brunt–Väiäslä frequency for the compressible system are defined as

$$b' = g \frac{\theta'}{\bar{\theta}}, \quad \text{and} \quad N^2 = \frac{g}{\bar{\theta}} \frac{d\bar{\theta}}{dz}.$$

Using the preceding expression for H, the second-order contributions to the pseudomomentum (18), and the pseudomomentum fluxes (26) and (27), become

$$P \approx \rho' u' + \bar{\rho}(z) \frac{\omega' b'}{N^2}, \tag{B2}$$

$$F_{(x)} \approx u_0 P + \frac{\bar{\rho}}{2} \left[(u')^2 - (w')^2 + \frac{(b')^2}{N^2} + \left(\frac{c_v}{R}\right)^2 c_s^2 \left(\frac{\pi'}{\bar{\pi}}\right)^2 \right], \tag{B3}$$

$$F_{(z)} \approx \bar{\rho} u' w'. \tag{B4}$$

To obtain solutions with sinusoidal vertical structure, the basic state is assumed isothermal and the perturbation variables are transformed, such that

$$(\tilde{u}, \tilde{w}, \tilde{\pi}, \tilde{b}) = \left(\frac{\bar{\rho}}{\rho_0}\right)^{1/2} (u', w', c_p \bar{\theta} \pi', b'),$$

where ρ_0 is a constant reference density.

Using the relation

$$\frac{\rho'}{\bar{\rho}} = \frac{c_v}{R} \frac{\pi'}{\bar{\pi}} - \frac{\theta'}{\bar{\theta}},$$

and the definition

$$\Gamma = -\frac{1}{2\bar{\rho}} \frac{d\bar{\rho}}{dz} - \frac{1}{\bar{\theta}} \frac{d\bar{\theta}}{dz},$$

the second-order approximations to the pseudomomentum and pseudomomentum fluxes, (B2)–(B4), may be reexpressed in terms of the transformed variables as

$$P = \rho_0 \left[\frac{\tilde{u} \tilde{\pi}}{c_s^2} + \frac{\tilde{b}}{N^2} \left(\frac{\partial \tilde{u}}{\partial z} + \Gamma \tilde{u} - \frac{\partial \tilde{w}}{\partial x} \right) \right], \tag{B5}$$

$$F_{(x)} = u_0 P + \frac{\rho_0}{2} \left[\tilde{u}^2 - \tilde{w}^2 + \frac{\tilde{b}^2}{N^2} + \frac{\tilde{\pi}^2}{c_s^2} \right]. \tag{B6}$$

$$F_{(z)} = \rho_0 \tilde{u} \tilde{w}. \tag{B7}$$

The group velocity must be obtained from the full dispersion relation for compressible flow. In the case of an isothermal basic state and constant mean flow u_0, wave solutions to the linearized governing equations exist of the form

$$\mathrm{Re}\{ e^{i(kx+mz-\hat{\nu}t)} \}$$

and satisfy the dispersion relation

$$\nu^4 - c_s^2 (k^2 + m^2 + \Gamma^2 + N^2/c_s^2) \nu^2 + N^2 c_s^2 k^2 = 0,$$

where $\nu = \hat{\nu} - u_0 k$ is the Doppler-shifted frequency. The horizontal and vertical components of the group velocity are thus

$$c_{g(x)} = \frac{\partial \hat{\nu}}{\partial k} = u_0 + \left(\frac{k}{\nu}\right) \frac{N^2 - \nu^2}{k^2 + m^2 + \Gamma^2 + N^2/c_s^2 - 2\nu^2/c_s^2}, \tag{B8}$$

and

$$c_{g(z)} = \frac{\partial \hat{\nu}}{\partial m} = -\frac{m\nu}{k^2 + m^2 + \Gamma^2 + N^2/c_s^2 - 2\nu^2/c_s^2}. \tag{B9}$$

To verify the group velocity condition, P, $F_{(x)}$, and $F_{(z)}$ need to be averaged over one phase of the wave. Choose the origin of the coordinate axis so that

$$\tilde{\pi} = \sin(kx + mz - \hat{\nu}t) \equiv \sin\phi;$$

then from the polarization relations

$$\tilde{u} = \frac{k}{\nu} \sin\phi,$$

$$\tilde{w} = \frac{\nu m}{\nu^2 - N^2} \sin\phi - \frac{\nu \Gamma}{\nu^2 - N^2} \cos\phi,$$

and

$$\tilde{b} = -\frac{mN^2}{\nu^2 - N^2} \cos\phi - \frac{\Gamma N^2}{\nu^2 - N^2} \sin\phi.$$

Substituting the preceding expressions into (B5)–(B7) and averaging over a phase of the wave, one obtains

$$\langle\langle P \rangle\rangle = \left(\frac{\rho_0 k}{2\nu}\right) \left[\frac{1}{c_s^2} + \frac{N^2}{(\nu^2 - N^2)^2} (m^2 + \Gamma^2) \right], \tag{B10}$$

$$\langle\langle F_{(x)} \rangle\rangle = u_0 \langle\langle P \rangle\rangle + \frac{\rho_0 k^2}{2\nu^2}, \tag{B11}$$

$$\langle\langle F_{(z)} \rangle\rangle = \left(\frac{\rho_0 k}{2}\right) \left(\frac{m}{\nu^2 - N^2}\right). \tag{B12}$$

The substitution of (B8)–(B12) into (B1) yields algebraic identities that verify the satisfaction of the group-velocity condition. Note that since this derivation used the unapproximated expressions for the group velocity in the compressible system, it was not necessary to distinguish sound waves from gravity waves, and thus, the group velocity condition is satisfied for either type of wave.

REFERENCES

Andrews, D. G., and M. E. McIntyre, 1978: On wave-action and its relatives. *J. Fluid Mech.,* **89,** 647–664.

Batchelor, G. K., 1967: *An Introduction to Fluid Dynamics.* Cambridge University Press, 615 pp.

Bretherton, F. P., 1966: The propagation of groups of internal gravity waves in a stratified shear flow. *Quart. J. Roy. Meteor. Soc.,* **92,** 466–480.

Durran, D. R., 1995: Do breaking mountain waves decelerate the local mean flow? *J. Atmos. Sci.,* **52,** 4010–4032.

Klemp, J. B., and D. R. Durran, 1983: An upper-boundary condition permitting internal gravity wave radiation in numerical mesoscale models. *Mon. Wea. Rev.,* **111,** 430–444.

Lilly, D. K., and J. B. Klemp, 1979: The effects of terrain shape on nonlinear hydrostatic mountain waves. *J. Fluid Mech.,* **95,** 241–261.

Littlejohn, R. G., 1982: Singular Poisson tensors. *Mathematical Methods in Hydrodynamics and Integrability in Dynamical Systems,* M. Tabor and Y. M. Treve, Eds., Amer. Inst. Phys. Conf. Proc., 47–66.

McIntyre, M. E., 1981: On the 'wave momentum' myth. *J. Fluid Mech.,* **106,** 331–347.

——, and T. G. Shepherd, 1987: An exact local conservation theorem for finite-amplitude disturbances to non-parallel shear flows, with remarks on Hamiltonian structure and on Arnold's stability theorems. *J. Fluid. Mech.,* **181,** 527–565.

Schar, C., 1993: A generalization of Bernoulli's theorem. *J. Atmos. Sci.,* **50,** 1437–1443.

Scinocca, J. F., and T. G. Shepherd, 1992: Nonlinear wave-activity conservation laws and Hamiltonian structure for the two-dimensional anelastic equations. *J. Atmos. Sci.,* **49,** 5–27.

——, and W. R. Peltier, 1994: Finite-amplitude wave-activity diagnostics for Long's stationary solution. *J. Atmos. Sci.,* **51,** 613–622.

Shepherd, T. G., 1990: Symmetries, conservation laws and Hamiltonian structure in geophysical fluid dynamics. *Advances in Geophysics,* Vol. 32, Academic Press, 287–338.

Whitham, G. B., 1974: *Linear and Nonlinear Waves.* John Wiley and Sons, 636 pp.